Iran University of Science and Technology

International Journal of

Railway Research

ISSN: 2423-3838

Volume-Filling Effects on Sloshing Frequency in Simplified and Explicit Dynamic Finite Element Models of Tank Wagons During Braking and Turning

A. Rahmati-Alaei[1*], M. Sharavi[2]

[1]Ph.D. Candidate, School of Railway Engineering, Iran University of Science and Technology

[2]Assistant Professor, School of Railway Engineering, Iran University of Science and Technology

ARTICLE INFO

Article history:
Received: 4 Mar. 2016
Accepted: 24 May 2016
Published: 21 Aug. 2016

Keywords:
Fluid sloshing
Explicit finite element model
Simplified sloshing model
Braking and turning

A B S T R A C T

Numerical analysis of fluid sloshing in tank wagons is amongst essential research ideas that are focused by railway engineers. The free surface of fluid becomes unstable and turns into a dynamic complex non-linear problem for fluid-structure interaction (FSI). In this paper, initially, the dynamic response of the tank, including lateral force analysis and pressure distribution during braking, is obtained by using an explicit dynamic finite element model based on the Multi Material Arbitrary Lagrangian Eulerian method (MM-ALE). Then, the simplified model is developed for sloshing during turning. Numerical finite element model is validated using a test setup. Comparing these models during turning with parametric studies for tank filling, it is observed that the estimated frequency and amplitude of sloshing, when filling is less than 25%, are less than 10% different form the measured results. Therefore, the simplified model in the above conditions can be used with an acceptable degree of accuracy. It also causes a remarkable reduction in the time and the cost of the numerical calculations.

1. Introduction

Every year, many accidents happen for tank wagons. When the tank wagon is half-full and the fluid inside it is freely in sloshing, the risk of derailment would be higher. In such problems, the fluid is under the influence of acceleration of external forces; as a result, the free surface of fluid becomes unstable. In the investigations of fluid-structures interaction (FSI), exact information about the behavior of free surface of fluid is a very important factor. Numerical simulation of fluid free-surface flow problems is based on solving complex partial differential equations of mass and momentum the so called Navier-Stokes equations. The Navier-Stokes equations on the discretized domain include millions of elements. The coupled non-linear equations are solved by iteration methods so that the velocity, pressure, and position of free surface are obtained on the discretized domain.

Lu et al. [1], Godderidge et al. [2-3], use the interface sharpening-global mass conservation (IS-GMC) method for Navier-Stokes equations. This method is based on the function of fluid free surface with two different values as the sign of free surface position. According to study of Liu et al. [4], Nicolici et al [5], Thiagarajan et al. [6], explicit finite element method can be used for solving these differential equations.

*Corresponding Author
Email Address: ahmad_rahmati@rail.iust.ac.ir
http:// tlx.doi.org/……..

Biswal et al. [7], Lin et al. [8]; Meddahi et al. [9], Kyoung et al. [10], analyze the sloshing using the finite element method. They found that the solution is close to the experimental data with high accuracy, but calculations of this method, especially for three-dimensional models, are time consuming. Mainly in this situation the simplified model has been used for a fast overview on sloshing response. In the simplified model, there is only one unknown for solving problems compared with millions of unknowns in finite element model. Therefore, this model is efficient and fast, but its' accuracy must be determined in different sloshing conditions.

In this paper, compared to Meddahi et al. [9], conditions in which the complex model of explicit dynamic finite element can be replaced by the simplified model are studied; therefore, there would be a remarkable decrease in the time and cost of calculations. As presented in Figure 1, in finite element model, sloshing of the fluid free-surface during braking and turning is first investigated. Then, by a parametric study of filling percentage in tanks, the accuracy of the simplified model is determined based on the frequency and amplitude of sloshing.

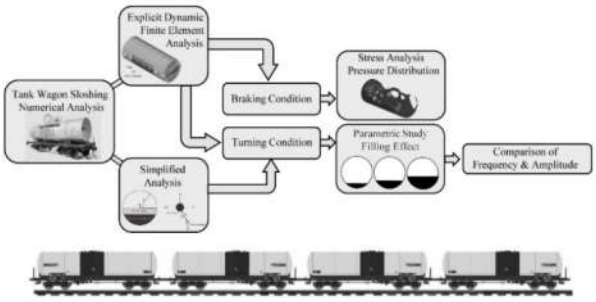

Figure 1: General process of modeling

2. Explicit Dynamic Finite Element Method

The non-inertial form of governing equations of sloshing in the explicit finite element method, named Navier-Stokes for Newtonian fluid, is as follows:

$$\rho(\frac{\partial u}{\partial t}+\mathrm{u}.\nabla \mathrm{u}) = -\rho \mathrm{N}+ \rho \mathrm{g}+\nabla.\sigma \quad (1)$$

$$N = \ddot{R} + 2\omega \times u + \dot{\omega} \times r + \omega \times \omega \times r \quad (2)$$

$$\sigma = -\mathrm{pl}+ 2\mu\varepsilon(u) \quad (3)$$

$$\nabla u = 0 \quad (4)$$

Where u, p, ρ, g, μ are respectively velocity, pressure, density, gravity acceleration, and dynamic viscosity. Strain tensor is $\varepsilon = \frac{1}{2}(\nabla u + \nabla u^T)$, and I stands for unit tensor.

Here, ω and $\dot{\omega}$ are respectively angular velocity and acceleration in the non-inertial form. R is the linear acceleration and r is the position vector (Figure 2).

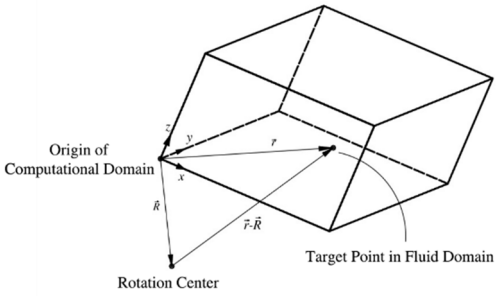

Figure 2: Non-inertial form in a three-dimensional tank

To simulate the problems of free-surface flow, it is assumed that the two fluids have minimal effects on each other. The free surface function of ϕ has two distinguished values (0, 1). Time-dependent advection equation transfers this function in the computational domain with fluid velocity. By using ϕ, density and viscosity can be calculated as:

$$\frac{\partial \phi}{\partial t} + u.\nabla \phi = 0 \quad (5)$$

$$\rho = \phi\mu_A + (1-\phi)\mu_B \quad (6)$$

$$\rho = \phi\rho_A + (1-\phi)\rho_B \quad (7)$$

Indices A and B demonstrate two different fluids. First, ø in fluid A is zero and in fluid B is 1. The explicit dynamic finite element method is used for solving equations of streamline-upwind/Petrov-Galerkin (SUPG) and pressure-stabilizing/Petrov-Galerkin (PSPG) techniques.

SUPG makes it possible to solve problems of free-surface flow at high velocities [11-12], and PSPG omits instabilities due to using linear interpolation functions for pressure and velocity.

In the explicit dynamic finite element method, first, suitable sets of protracted response spaces of S_u^h , S_p^h , and S_ϕ^h as well as weight function spaces of V_u^h , V_p^h , and V_ϕ^h are defined for velocity, pressure, and free-surface functions, respectively. Therefore, Equations (1) and (2) can be written and for all $q^h \in V_p^h, w^h \in V_u^h$ and $\varphi^h \in V_\phi^h$, values of $p^h \in S_p^h, u^h \in S_u^h$ and $\phi^h \in S_\phi^h$ are obtained as follows:

$$\begin{aligned}
&\left[\rho\left[\frac{\partial u^h}{\partial t}+u^h.\nabla u^h-g+N\right]-\nabla.\sigma(\mathrm{p}^h,\mathrm{u}^h)\right]d\Omega\\
&\int_\Omega \varepsilon(\omega^h).\sigma(\mathrm{p}^h,\mathrm{u}^h)d\Omega+\int_\Omega q_p^h\nabla.u^h d\Omega\\
&+\int_\Omega \psi^h(\frac{\partial \phi^h}{\partial t}+\mathrm{u}^h.\nabla\phi^h)d\Omega+\sum_{e=1}^{ne}\int_{\Omega^e}\tau_c\nabla u^h d\Omega\\
&+\sum_{e=1}^{ne}\int_{\Omega^e}\frac{\tau_m}{\rho}\left[u^h.\nabla w^h-\nabla.\sigma(\mathrm{q}_p^h,\mathrm{w}^h)\right]\\
&\int_\Omega w^h.\rho\left[\frac{\partial u^h}{\partial t}+u^h.\nabla u^h-g-N\right]d\Omega+\\
&+\sum_{e=1}^{ne}\int_{\Omega^e}\tau_i\nabla\psi^h.\nabla\phi^h d\Omega=\int_{\Gamma_{hu}} w^h.hd\Gamma
\end{aligned} \tag{8}$$

Parameters of τ_m, τ_c , and τ_i are stability parameters:

$$\tau_c=\frac{h}{2}\|u\|z \quad , \quad z=\begin{cases}R_u/3 & R_u\le 3\\ 1 & R_u\end{cases} \tag{9}$$

$$\tau_i=\frac{h}{2}\|u\| \tag{10}$$

$$\tau_m=\left[(\frac{2\|u\|}{h})^2+(\frac{4u}{\rho h})^2\right] \tag{11}$$

Here, h is element length and R_u is cell Reynolds number.

In Equation (8), the first four integral terms and the integral on the right of the equal sign show Galerkin relations of equations. Terms of the first, second, and third series are respectively least square of continuum equation, SUPG stability for momentum equations, and stability of artificial diffusion for surface function. Diffusion relations for surface function omit the low (below 0) and high (above 1) estimations of the function from the whole surface. In the IS-GMC algorithm, interface sharpening is improved in such a way that fluid mass conservation is established locally and generally.

Discretizing of explicit dynamic finite element equations leads to a series of coupled nonlinear equations which need to be solved in every time step. First, the obtained equations linearized by Newton-Raphson method; then, the series obtained from the linear equations is solved by iteration and the generalized minimal residual algorithm [13]. For very large systems, matrix-free iteration technique is used to find the response of linear system [14]. These vector-elements calculations totally omit the need for any type of matrix, even in the element surface.

2.1. Numerical Modeling

In this section, the sloshing of the tank wagon during braking is simulated by a three-dimensional model using numerical hydro-code LS-DYNA. In the tank wagon demonstrated in Figure 3, it is assumed that the liquid fills half of the tank with a circular cross-section, and is moving at the velocity of 10 m/s. Discretizing of computational domain is demonstrated in Figure 3(a). The mesh used in this analysis has three parts of air, fluid (water), and tank, and includes 12000 shell elements with Belytschko-Tsay formulation and 132000 solid elements.

The numerical method used here is Multi Material Arbitrary Lagrangian Eulerian method (MM-ALE). According to this method which is based on a unique continuum mechanic formulation, when changes in Lagrangian elements are more than a certain level, materials are moved in the cells by Euler method and a Lagrangian new meshing is generated in the new place of the material. Therefore, one can utilize the unique capability of Euler method for changing very large forms and predicting boundary of materials with enough accuracy. Air is modeled by Null material model and an equation of state as follows:

$$P=C_0+C_1\mu+C_2\mu^2+C_3\mu^3+(\mathrm{C}_4+\mathrm{C}_5+\mathrm{C}_6\,\mu^2)\mathrm{E} \tag{12}$$

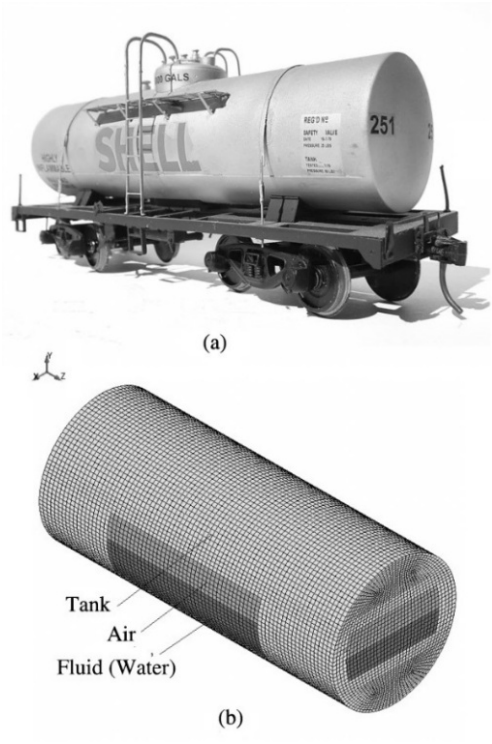

Figure 3: Tank wagon; (a) Real case. (b) Finite element model

In which $\mu = \frac{\rho}{\rho_0} - 1$ ρ , ρ_0 , E, and C_0 to C_6 parameters are density, nominal density, initial internal energy, and equation coefficients, respectively. For water, Gruneisen equation of state is used [15]. The Gruneisen equation of state with cubic shock velocity-particle velocity defines pressure for compressed materials as:

$$P = \frac{\rho_0 C^2 \mu \left[1 + \left(1 - \frac{\gamma_0}{2}\right)\mu - \frac{a}{2}\mu^2\right]}{\left[1 - (S_1 - 1)\mu - S_2 \frac{\mu^2}{\mu + 1} - S_3 \frac{\mu^3}{(\mu + 1)^2}\right]^2} + (\gamma_0 + a\,\mu)E \quad (13)$$

Where C, a, S1 to S3 respectively are volume speed sound, volumetric correction factor, and coefficients of slope of the curve $v_s - v_p$ (shock wave speed-particle rate). Table 1 demonstrates the coefficients of material model.

Table 1. Material Model

Air	ρ (kg/m^3)	C_0	C_1	C_2	C_3	C_4	C_5	$E_0(J/m^3)$
	1.29	0	0	0	0	0.4	0.4	2.5×10^5
Water	ρ (kg/m^3)	$C_0(m/s)$	S_1	S_2	S_3	γ_0	a	$E_0(J/m^3)$
	1000	1483	1.7	0.09	0	0.2	0	0

2.2. Tank Sloshing in Braking

Here, it is assumed that tank speed slows down by 0.25g. Fluid starts sloshing and generates oscillation force along the length of tank wagon. In each nonlinear iteration, equations are solved by almost 2 million unknowns so that a transient response would be obtained. Figure 4(a) and Figure 4(b) demonstrate forces imposed on the tank cross-section in longitudinal and gravity directions, respectively, with deformation of the cross section. Because of negative braking acceleration, vertical force peak occurs when the fluid reaches the tank cross-section at 30ms, and it is damped after 600ms. After 30ms, the section curve starts decreasing and reaches its initial state at 500ms. The force of y direction still has consecutive peaks and is not yet damped, because gravity acceleration is imposed and there is sloshing in vertical direction with the maximum value of 48kN.

Figure 5 demonstrates pre- and post-braking pressure distribution. Fluid pressure is highly variable in every time step. Because of the negative braking acceleration of fluid, first there is longitudinal sloshing along the tank section which reaches the opposite section when the tank is half-filled. According to the figure, maximum instabilities in fluid sloshing occur at 500ms and the approximate amplitude of 0.48-1.2MPa; after the damping of sloshing impulse force, the free surface of fluid will reach its initial stable state.

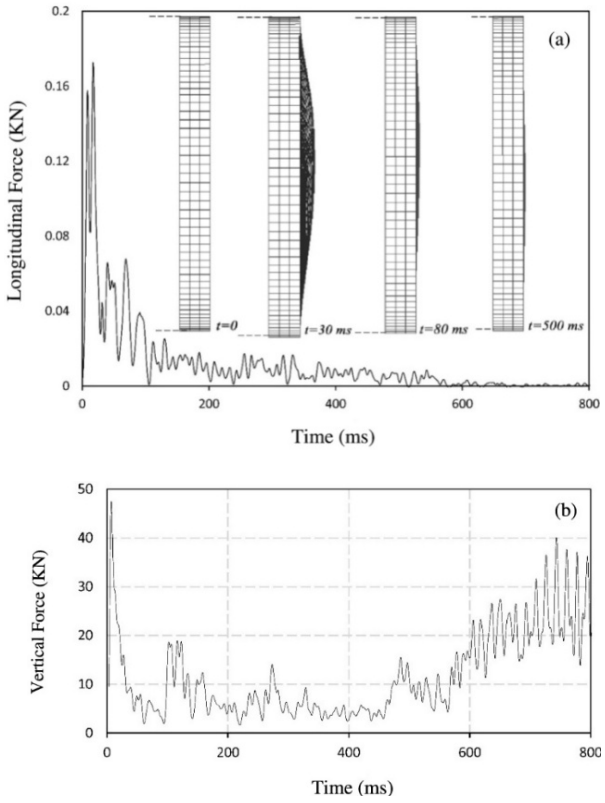

Figure 4: Force imposed on the tank in braking; a) longitudinal direction. b) gravity direction

The numerical finite element model is validated using a test setup made by Sharavi et al. [16-17] by image processing method. The video camera records the image of fluid sloshing from the instant of releasing the weight until after the impact and the disappearance of sloshing. Free surface profile of test and numerical models at different times have a similar shape and have been compared in Figure 6.

According to the previous study of author (Sharavi et al, 2015), the displacement of center of mass for fluid tank are shown in Figure 7. It is obvious that the finite element method and the test have a considerable agreement and differ by less than 10%.

3. The Simplified Method

In the simplified model, the obtained values are the sum of the sloshing part and the fixed liquid part. The fluid is assumed to be in the form of a lumped mass connected to a link with the length of R [18]. The lumped mass is connected to the non-inertial frame with a frictionless joint at point "O" (Figure 8). Equations of motion are as follows:

$$\frac{d\omega}{dt} = \frac{1}{R}(a\cos\theta - g\sin\theta) \tag{14}$$

$$\frac{d\theta}{dt} = \omega \tag{15}$$

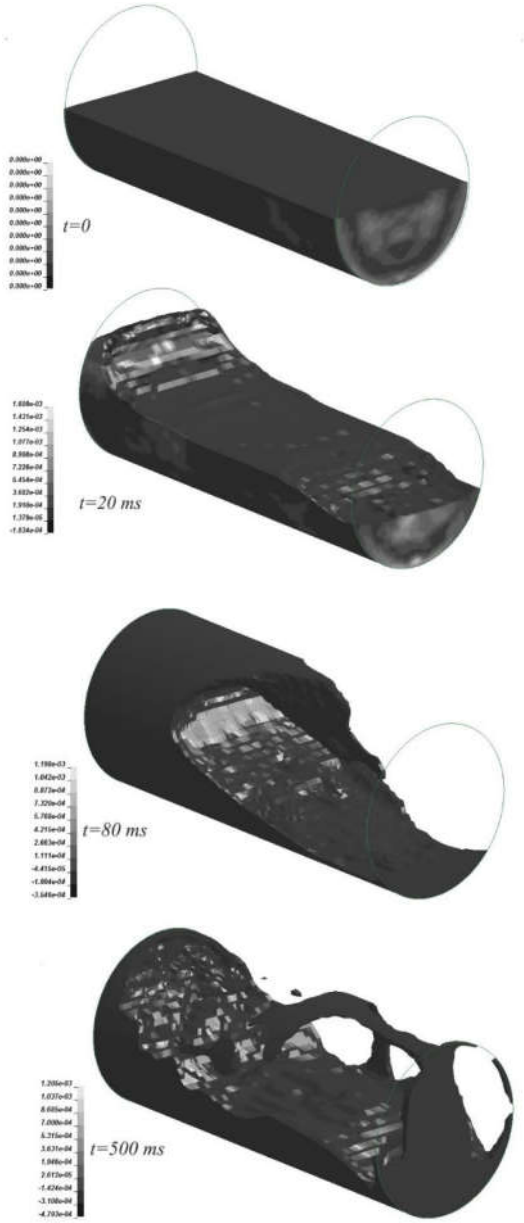

Figure 5: Pressure distribution in braking (GPa)

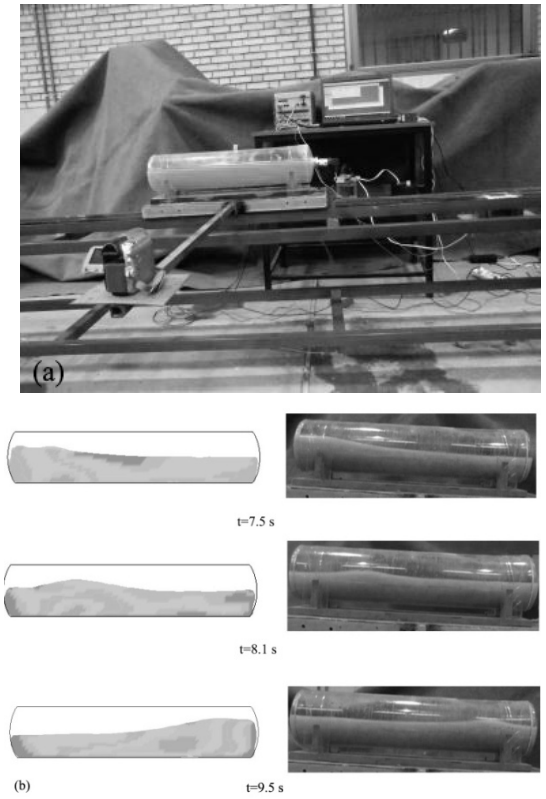

Figure 6: Tank sloshing; a) test setup. b) Free surface profile; 50% filling.

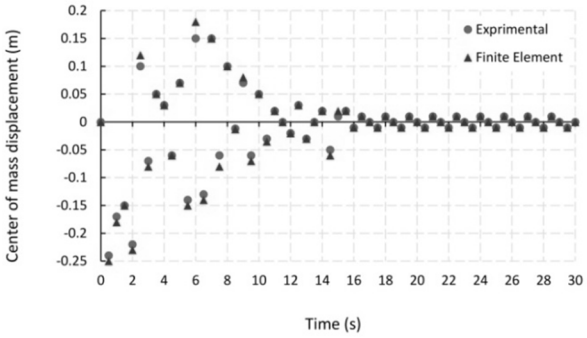

Figure 7: Center of mass displacement in the direction of tank motion by test and finite element model

Whereθ is the relative vertical angle, ω is the angular speed, and α and g are the horizontal and vertical accelerations, respectively. The initial conditions for Equations (14) and (15) are:

$$\theta|_{t=0} = 0, \quad , \ \omega|_{t=0} = 0 \tag{16}$$

By integrating the equations, the following equations will be obtained with second-order accuracy. Index "n" is the counter of time step and is the time step:

$$\theta^{n+1} = \theta^n + \frac{\Delta t}{2}\left[\omega^{n+1} + \omega^n\right] \tag{17}$$

$$\omega^{n+1} = \omega^n + \frac{\Delta t}{2}\left[\frac{1}{R}(a\cos\theta^{n+1} - g\sin\theta^{n+1}) + \frac{1}{R}(a\cos\theta^n - g\sin\theta\right] \tag{18}$$

By combining Equations (17) and (18), the following equation can be obtained:

$$\theta^{n+1} = \theta^n + \Delta t\,\omega^n + \frac{(\Delta t)^2}{4}\left[\frac{1}{R}(a\cos\theta^{n+1} - g\sin\theta^{n+1}) + \frac{1}{R}(a\cos\theta^n - g\sin\theta^n)\right] \tag{19}$$

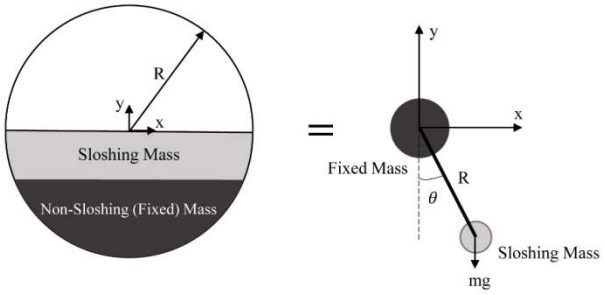

Figure 8: The simplified model

In these equations, θ^{n+1} is the only unknown, which is obtained by Newton-Raphson linearization algorithm. For the complete modeling of sloshing, the model must have infinite oscillating masses, in which each mass corresponds to one of the sloshing modes. Therefore, the above simplified model is acceptable as long as excitation frequency is not close to the natural frequencies of higher modes of sloshing. Of course sometimes when the second mode frequency gets close to the main mode frequency or there is high mass sloshing, calculations related to the second mode must also be performed. If the calculations of force and moment are available, sloshing parameters are directly found accordingly.

3.1. Tank Sloshing in Turning

To evaluate the accuracy of the simplified model, fluid sloshing of the tank in turning is considered. Radial acceleration is equal to the centrifugal acceleration in the tank wagon. If the speed of the

tank wagon and curve radius are v and r respectively, then:

$$a = \frac{v^2}{r} \tag{20}$$

Using finite element and simplified analysis, numerical simulation is performed for a tank wagon with circular cross-section and horizontal acceleration of $0.04g$. There are standards for the level of filling of a tank wagon. For example, the ASME Section VIII [19] can be mentioned. In Figure 9, obtained results for finite element model and simplified model for the filling percentages of P=45%, P=25%, and P=15% are represented. Here, the comparison is based on dimensionless radial force $F/\rho g L^2$ imposed on the tank based on dimensionless time $t\sqrt{R/g}$ during turning.

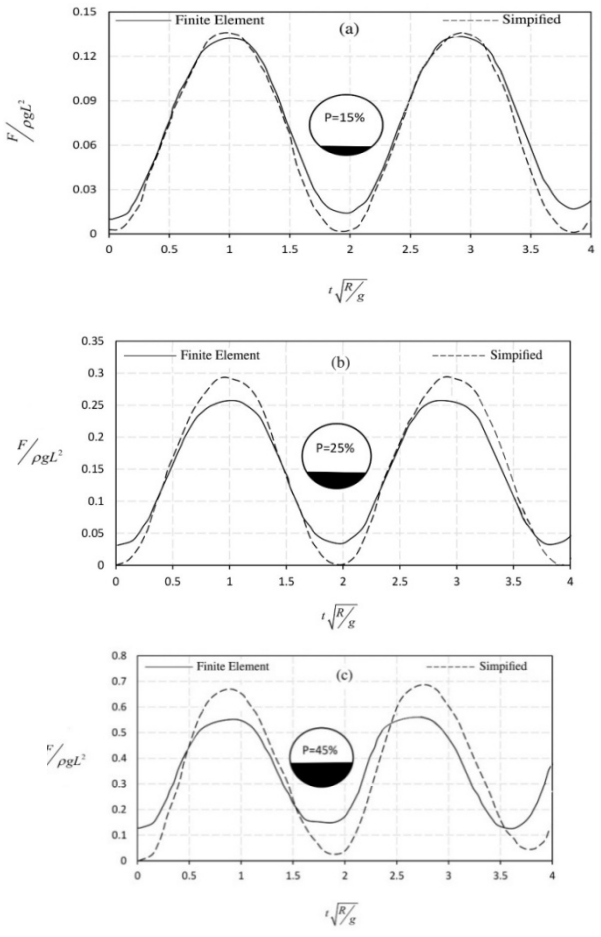

Figure 9: Radial force of the tank with different filling percentages; (a) 15% (b) 25% (c) 45%

According to Figure 9, when the amount of fluid in the tank is low (P = 15%), force amplitudes have the difference of less than 10%. Based on Figure 10, the sloshing frequency by almost 5% difference is the same for both models with low and moderate height of fluid (P = 15%, P = 25%). According to Figure 9(c) and Figure 10, when there is remarkable volume of fluid in the tank (P = 45%), the difference between force amplitude and sloshing frequency in the two models will sharply increase. Therefore, the simplified model can replace the explicit dynamic finite element model when the filling percentage is less than 25%, and can remarkably decrease calculation cost and time.

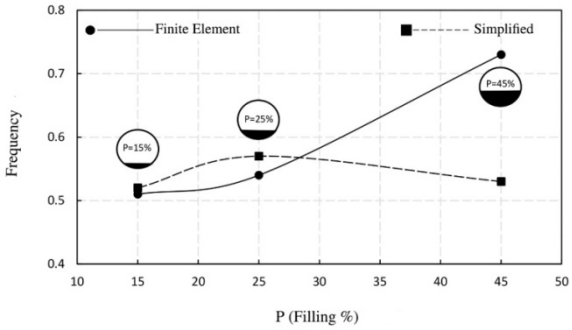

Figure 10: Sloshing frequency at different filling percentages

4. Conclusions

In this paper, the numerical analysis of explicit dynamic finite element and the simplified model were used for simulating sloshing in tank wagons during braking and turning. Due to negative braking acceleration, the fluid had longitudinal sloshing along the tank section at first and, when the tank was half-filled, it reached the opposite section; therefore, the maximum sloshing instability of the fluid free-surface occurred at 500ms. Afterwards, the normal force peak of the tank section became zero. For sloshing in turning, the results obtained from simplified and explicit dynamic finite element methods are close at low and average filling (P = 15%, P = 25%). Precisely, at the filling percentage of less than 25%, sloshing frequency and force amplitude had less than 5% and 10% difference, respectively. Therefore, in such conditions, the simplified model can be used instead of the complex explicit dynamic finite element model in order to remarkably decrease the time and cost of calculations.

List of symbols

g	gravitational acceleration
h	length of the element
I	unit tensor
p	pressure
r	distance between the origin and the target points
R	distance between the origin and the rotation center
R_u	Reynolds number
t	flow time
u	flow velocity
ρ	density
ω	angular velocity
μ	dynamic viscosity
ε	rate of strain tensor
ϕ	free surface function
τm, τc, τi	stability parameters
∇	divergence

References

[1] L. Lu, Sc. Jiang, M. Zhao and Gq Tang, Two-dimensional viscous numerical simulation of liquid sloshing in rectangular tank with/without baffles and comparison with potential flow solutions, Ocean Engineering 108 (2015): 662-677.

[2] B. Godderidge, S.R. Turnock and M. Tan., Evaluation of a rapid method for the simulation of sloshing in rectangular and octagonal containers at intermediate filling levels, Computers & Fluids 57 (2012): 1-24.

[3] B. Godderidge, S. Turnock, C. Earl and M. Tan, The effect of fluid compressibility on the simulation of sloshing impacts, Ocean Engineering 36.8 (2009): 578-587.

[4] D. Liu, P. Lin., A numerical study of three-dimensional liquid sloshing in tanks, Journal of Computational physics 227.8 (2008): 3921-3939.

[5] S. Nicolici, R. M. Bilegan, Fluid structure interaction modeling of liquid sloshing phenomena in flexible tanks, Nuclear Engineering and Design 258 (2013): 51-56.

[6] K. P. Thiagarajan, D. Rakshit and N. Repalle, The air–water sloshing problem: Fundamental analysis and parametric studies on excitation and fill levels, Ocean Engineering 38.2 (2011): 498-508.

[7] K. C. Biswal, S. K. Bhattacharyya, Dynamic response of structure coupled with liquid sloshing in a laminated composite cylindrical tank with baffle, Finite Elements in Analysis and Design 46.11 (2010): 966-981.

[8] G. Lin, J. Liu, J. Li and Z. Hu, A scaled boundary finite element approach for sloshing analysis of liquid storage tanks, Engineering Analysis with Boundary Elements 56 (2015): 70-80.

[9] S. Meddahi, D. Mora and R. Rodríguez, Finite element analysis for a pressure–stress formulation of a fluid–structure interaction spectral problem, Computers & Mathematics with Applications 68.12 (2014): 1733-1750.

[10] J. H. Kyoung, S. Y. Hong, J. W. Kim and K. J. Bai, Finite-element computation of wave impact load due to a violent sloshing, Ocean engineering 32.17 (2005): 2020-2039.

[11] S. Aliabadi, A. Johnson and J. Abedi, Comparison of finite element and pendulum models for simulation of sloshing, Computers & Fluids 32.4 (2003): 535-545.

[12] P. Pal, S. K. Bhattacharyya, Sloshing in partially filled liquid containers—Numerical and experimental study for 2-D problems, Journal of Sound and Vibration 329.21 (2010): 4466-4485.

[13] Y. Saad, M. H. Schultz, GMRES: A generalized minimal residual algorithm for solving nonsymmetric linear systems, SIAM Journal on scientific and statistical computing 7.3 (1986): 856-869.

[14] O. M. Faltinsen, A. N. Timokha, Analytically approximate natural sloshing modes and frequencies in two-dimensional tanks, European Journal of Mechanics-B/Fluids 47 (2014): 176-187.

[15] J. O. Hallquist, LS-DYNA keyword user's manual, Livermore Software Technology Corporation 970 (2007).

[16] M. Shahravi, M. R. Sajjadi and M. M. Feizi, Investigation of sloshing coefficient by arbitrary Lagrange-Euler methods in partially filled tankers, Advances in Railway Engineering, An International Journal 2.1 (2014): 1-11.

[17] R. Razaghi, M. Sharavi and M. M. Feizi., Investigating the effect of sloshing on the energy absorption of tank wagons crash, Transactions of the Canadian Society for Mechanical Engineering 39.2 (2015): 187.

[18] R. A. Ibrahim, Liquid sloshing dynamics: theory and applications, Cambridge University Press, (2005).

[19] ASME, Boiler and Pressure Vessel Code, Division 1, Section III, Appendix F (2004).